Two-Photon Absorption in Quadrupolar Bis(acceptor)-Terminated Chromophores with Electron-Rich Bis(heterocycle)vinylene Bridges

ARTICLE *in* CHEMISTRY OF MATERIALS · FEBRUARY 2007

Impact Factor: 8.35 · DOI: 10.1021/cm0616811

Two-Photon Absorption in Quadrupolar Bis(acceptor)-Terminated Chromophores with Electron-Rich Bis(heterocycle)vinylene Bridges

Shijun Zheng,[†] Amalia Leclercq,[†] Jie Fu,[‡] Luca Beverina,[†] Lazaro A. Padilha,[‡,§] Egbert Zojer,[†,||] Karin Schmidt,[†] Stephen Barlow,[†] Jingdong Luo,[⊥] Sei-Hum Jiang,[⊥] Alex K.-Y. Jen,[⊥] Yuanping Yi,[#] Zhigang Shuai,[#] Eric W. Van Stryland,[‡,¶] David J. Hagan,[‡,¶] Jean-Luc Brédas,[†] and Seth R. Marder*[,†]

School of Chemistry and Biochemistry, Georgia Institute of Technology, Atlanta, Georgia 30332-0400, CREOL, The College of Optics and Photonics, University of Central Florida, Orlando, Florida 32816-2700, Institute of Solid-State Physics, Graz University of Technology, Petergasse 16, A-8010 Graz, Austria, Materials Science and Engineering Department, University of Washington, Seattle, Washington 98195, and Key Laboratory of Organic Solids, Institute of Chemistry, The Chinese Academy of Sciences, 100080 Beijing, P. R. China

Received July 19, 2006. Revised Manuscript Received November 6, 2006

Two-photon absorption spectra for a range of bis(acceptor)-substituted bis(dibutoxythienyl)ethene and bis(*N*-hexylpyrrolyl)ethene chromophores have been recorded using Z-scan and white-light-continuum pump−probe techniques. All the chromophores studied show strong near-infrared two-photon absorption with cross sections in the range of 2400−5900 GM (1 GM = 1×10^{-50} cm^4 s/photon) at photon wavelengths between 1.0 and 1.3 μm; cross sections as high as 10000 GM can be accessed close to the one-photon absorption edge. Quantum-chemical calculations reproduce the experimentally observed variations of the two-photon properties with the chemical structure.

Introduction

Two-photon absorption (2PA) processes are currently of great interest for applications including three-dimensional (3D) fluorescence imaging,[1,2] photodynamic therapy,[3] optical pulse supression,[4] and 3D microfabrication.[5−7] In order to realize the full potential of these applications, substantial efforts have been directed at understanding the molecular design principles necessary to develop chromophores with large 2PA cross sections, δ, at a range of visible and near-infrared (NIR) wavelengths. Dipolar,[8,9] quadrupolar,[10,11] and octupolar molecules[12,13] have been investigated both experimentally and theoretically. More complex systems investigated include dendritic species[14,15] and porphyrin oligomers and polymers.[16] In quadrupolar conjugated systems, the low-energy peak two-photon cross section, δ_{max}, seems to be related to symmetric charge transfer associated with the one-photon excitation. Thus, donor−bridge−donor (D−π−D) chromophores show higher δ_{max} values than the corresponding unsubstituted counterparts,[10] with even higher values (and a red-shifted 2PA maximum) observed in species with longer π-bridges[12,17] or in species with acceptor groups on the π-bridge (D−A−D).[10,17,18] Large δ values can also be obtained when the sense of quadrupolar charge transfer is reversed in A−π−A or A−D−A structural motifs.[10,17−20] Representative examples are shown in Figure 1.

* Corresponding author.
[†] Georgia Institute of Technology.
[‡] CREOL.
[§] Permanant address: Instituto de Física, UNICAMP, Campinas, Brazil.
[||] Graz University of Technology.
[⊥] University of Washington.
[#] Chinese Academy of Sciences.
[¶] Also with the Department of Physics, University of Central Florida.

(1) Denk, W.; Strickler, J. H.; Webb, W. W. *Science* **1990**, *248*, 73.
(2) So, P. T. C.; Dong, C. Y.; Masters, B. R.; Berland, K. M. *Annu. Rev. Biomed. Eng.* **2000**, *2*, 399.
(3) Fisher, W. G.; Partridge, W. P., Jr.; Dees, C.; Wachter, E. A. *Photochem. Photobiol.* **1997**, *66*, 141.
(4) Spangler, C. W. *J. Mater. Chem.* **1999**, *9*, 2013.
(5) Strickler, J. H.; Webb, W. W. *Proc. SPIE* **1990**, *1398*, 107.
(6) Maruo, S.; Nakamura, O.; Kawata, S. *Opt. Lett.* **1997**, *22*, 132.
(7) Cumpston, B. H.; Ananthavel, S. P.; Barlow, S.; Dyer, D. L.; Ehrlich, J. E.; Erskine, L. L.; Heikal, A. A.; Kuebler, S. M.; Lee, I.-Y. S.; McCord-Maughon, D.; Qin, J.; Röckel, H.; Rumi, M.; Wu, X.-L.; Marder, S. R.; Perry, J. W. *Nature* **1999**, *398*, 51.
(8) Belfield, K. D.; Hagan, D. J.; Van, Stryland, E. W.; Schafer, K. J.; Negres, R. A. *Org. Lett.* **1999**, *1*, 1575.
(9) Antonov, L.; Kamada, K.; Ohta, K.; Kamounah, F. S. *Phys. Chem. Chem. Phys.* **2003**, *5*, 1193.
(10) Albota, M.; Beljonne, D.; Brédas, J.-L.; Ehrlich, J. E.; Fu, J.-Y.; Heikal, A. A.; Hess, S. E.; Kogej, T.; Levin, M. D.; Marder, S. R.; McCord-Maughon, D.; Perry, J. W.; Röckel, H.; Rumi, M.; Subramaniam, G.; Webb, W. W.; Wu, X.-L.; Xu, C. *Science* **1998**, *281*, 1653.
(11) Ventelon, L.; Moreaux, L.; Mertz, J.; Blanchard-Desce, M. *Chem. Commun.* **1999**, 2055.
(12) Cho, B. R.; Son, K. H.; Lee, S. H.; Song, Y.-S.; Lee, Y.-K.; Jeon, S.-J.; Choi, J. H.; Lee, H.; Cho, M. *J. Am. Chem. Soc.* **2001**, *123*, 10039.
(13) Beljonne, D.; Wenseleers, W.; Zojer, E.; Shuai, Z.; Vogel, H.; Pond, S. J. K.; Perry, J. W.; Marder, S. R.; Brédas, J.-L. *Adv. Funct. Mater.* **2002**, *12*, 631.
(14) Chung, S.-J.; Kim, K.-S.; Lin, T.-C.; He, G. S.; Swiatkiewicz, J.; Prasad, P. N. *J. Phys. Chem. B* **1999**, *103*, 10741.
(15) Drobizhev, M.; Karotki, A.; Dzenis, Y.; Rebane, A.; Suo, Z.; Spangler, C. W. *J. Phys. Chem. B* **2003**, *107*, 7540.
(16) Drobizhev, M.; Stepanenko, Y.; Dzenis, Y.; Karotki, A.; Rebane, A.; Taylor, P. N.; Anderson, H. L. *J. Am. Chem. Soc.* **2004**, *126*, 15352.
(17) Rumi, M.; Ehrlich, J. E.; Heikal, A. A.; Perry, J. W.; Barlow, S.; Hu, Z.; McCord-Maughon, D.; Parker, T. C.; Röckel, H.; Thayumanavan, S.; Marder, S. R.; Beljonne, D.; Brédas, J.-L. *J. Am. Chem. Soc.* **2000**, *122*, 9500.
(18) Pond, S. J. K.; Rumi, M.; Levin, M. D.; Parker, T. C.; Beljonne, D.; Day, M. W.; Brédas, J.-L.; Marder, S. R.; Perry, J. W. *J. Phys. Chem. A* **2002**, *106*, 11470.
(19) Halik, M.; Wenseleers, W.; Grasso, C.; Stellacci, F.; Zojer, E.; Barlow, S.; Brédas, J. L.; Perry, J. W.; Marder, S. R. *Chem. Commun.* **2003**, 1490.

10.1021/cm061681l CCC: $37.00
Published on Web 01/13/2007

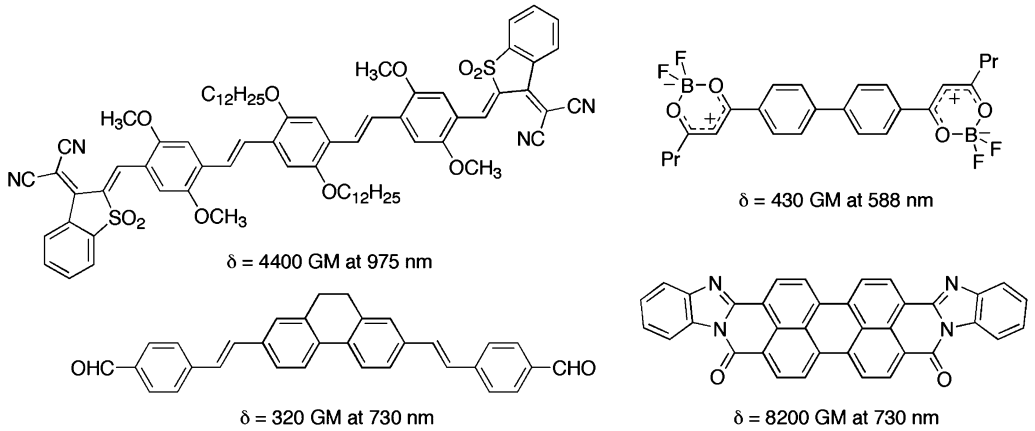

Figure 1. Some examples of quadrupolar (or approximately quadrupolar) A−π−A and A−D−A 2PA chromophores described in the literature with the maximum cross sections reported along with the corresponding wavelengths.

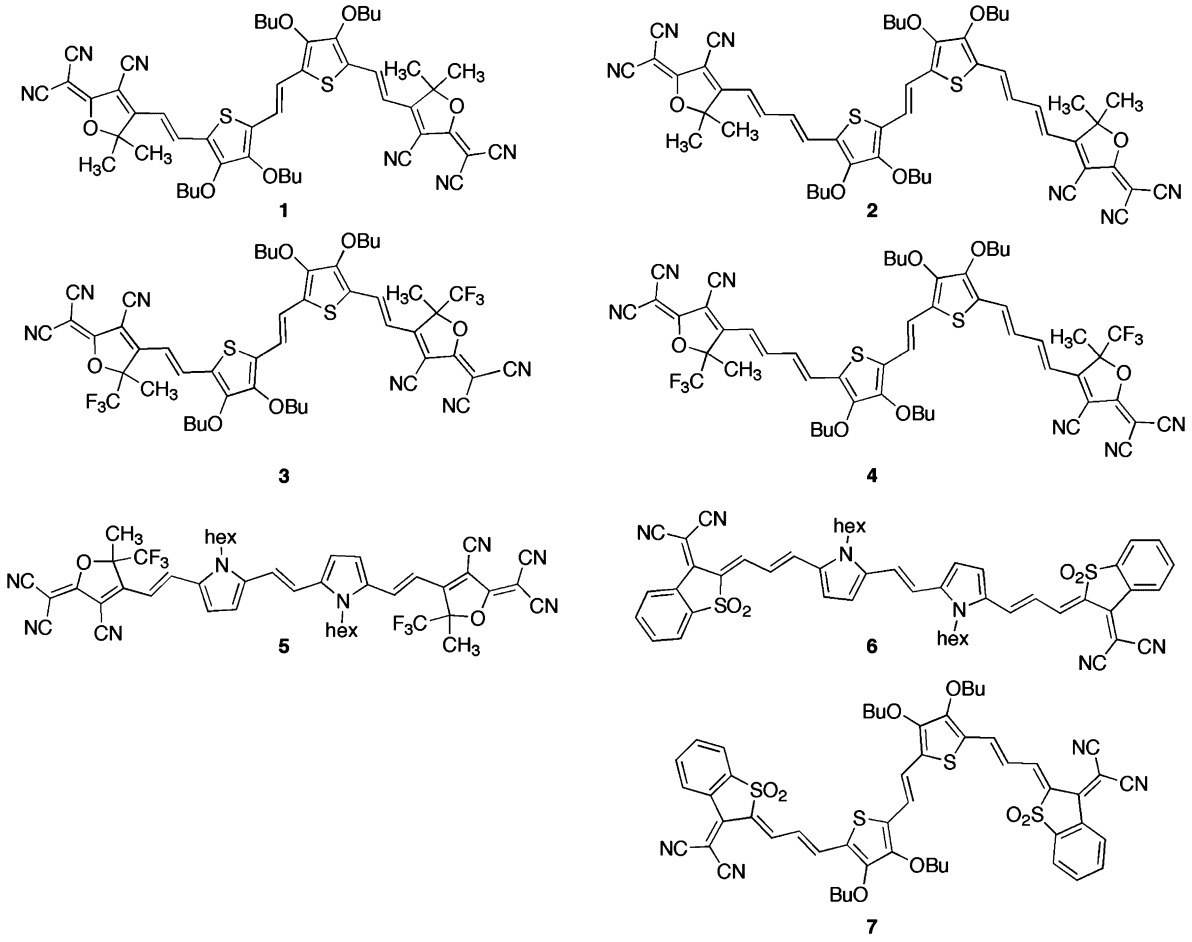

Figure 2. Structures of the chromophores considered in this paper.

In this paper, we present a joint experimental and theoretical 2PA study of new A−D−A chromophores in which strong acceptor end groups are conjugated through polyene linkages to *E*-1,2-bis(3,4-dibutoxythien-2-yl)ethylene and *E*-1,2-bis(*N*-hexylpyrol-2-yl)ethylene donor cores. The chromophores examined (**1**−**7**) are shown in Figure 2. Specifically, the three acceptor groups used are 4,5,5-trimethyl-3-cyano-2(5H)-furanylidenepropanedinitrile (the so-called "TCF" acceptor group, used in **1** and **2**), 4,5-dimethyl-5-trifluoromethyl-3-cyano-2(5H)-furanylidenepropanedinitrile (the so-called "CF_3−TCF" acceptor group, used in **3**−**5**), and 3-dicyanomethylidene-2,3-dihydrobenzothiophene-1,1-dioxide (which has previously been referred to as the "SDS" acceptor, used in **6** and **7**); all three of these have been previously shown to act as strong acceptor groups in dipolar second-order nonlinear optical (NLO) chromophores.[21−23]

(20) Oliveira, S. L.; Corrêa, D. S.; Misoguti, L.; Constantino, C. J. L.; Aroca, R. F.; Zilio, S. C.; Mendonça, C. R. *Adv. Mater.* **2005**, *17*, 1890.

(21) Shi, Y.; Zhang, C.; Zhang, H.; Bechtel, J. H.; Dalton, L. R.; Robinson, B. H.; Steier, W. H. *Science* **2000**, *288*, 119.

(22) Liu, S.; Haller, A.; Ma, H.; Dalton, L. R.; Jang, S.-H.; Jen, A. K.-Y. *Adv. Mater.* **2003**, *15*, 605.

Scheme 1

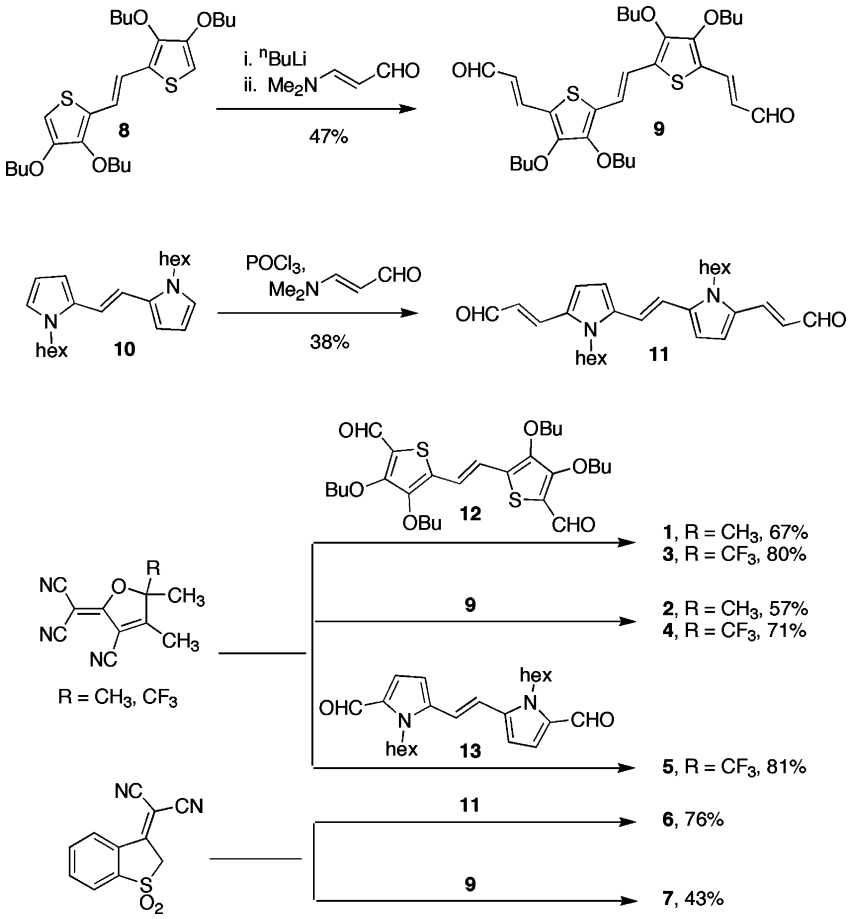

Results and Discussion

Synthesis. Chromophores **1**−**7** were synthesized in good yields by Knoevenagel condensation of the corresponding dialdehydes with the acceptor groups under microwave-promoted conditions (Scheme 1). Dialdehyde **9** was prepared by lithiation of *E*-bis(dibutoxythienyl)ethylene, **8**, followed by quenching with *N*,*N*-dimethylacrolein, while **11** is obtained from the reaction of *E*-bis(hexylpyrrolyl)ethylene, **10**, and *N*,*N*-dimethylacrolein under Vilsmeier conditions. Compounds **8**, **10**, **12**, and **13** and the three acceptors were synthesized according to, or in analogy to, the literature procedures.[24−27]

Electrochemistry. Cyclic voltammograms of **1**−**7** were measured in solutions of dichloromethane with 0.1 M tetra(*n*-butyl)ammonium hexafluorophosphate as electrolyte; the data are summarized in Table 1. The values for the potentials $E_{1/2}^{+/0}$, corresponding to the half-wave potentials for one-electron oxidation from the chromophore to its radical cation, indicate that the pyrrole chromophores are more easily oxidized than their thiophene analogues (**6** vs **7**; **5** vs **3**).

Table 1. Solution Half-Wave Redox Potentials, $E_{1/2}$ (V vs $FeCp_2^{+/0}$), from Cyclic Voltammetry (CH_2Cl_2, 0.1 M [$^nBu_4N$][PF_6], 50 mV s^{-1}) for 1−7

	$E_{1/2}^{2+/+}$	$E_{1/2}^{+/0}$	$E_{1/2}^{0/-}$	$E_{1/2}^{-/2-}$
1	nvm[c]	+0.73	−0.80[a]	
2	+0.73	+0.47	−0.79[a]	
3	nvm[c]	+0.80	−0.59[a]	
4	+0.78	+0.53	−0.62[a]	
5	+0.77	+0.52	−0.76	−1.12
6	+0.67	+0.33	−0.78	−0.92
7	+0.95[b]	+0.65	−0.62[a]	

[a] Two overlapping one-electron processes. [b] Irreversible, value given is peak potential, E_{ox}. [c] No value measured.

Moreover, the *shift* in $E_{1/2}^{+/0}$ between the parent bis(pyrrolyl)ethylene, **10**, and the acceptor-substituted derivatives **5** (+0.56 V) and **6** (+0.37 V) is greater than that between the parent bis(dialkoxythienyl)ethylene, **8**, and **3** (+0.44 V) and **7** (+0.29 V), respectively,[28] suggesting that substitution with a given acceptor has a greater effect on the donor core in the case of the bis(pyrrolyl)ethylene core, consistent with greater contributions from charge-separated resonance structures in the ground state of **5** and **6** relative to those in **3** and **7**, respectively. In addition, $E_{1/2}^{0/-}$ values indicate that the pyrrole chromophores are less readily reduced than their thiophene analogues, indicating the acceptor portions of the pyrrole-based chromophores to be less electron-poor than

(23) Ahlheim, M.; Barzoukas, M.; Bedworth, P. V.; Blanchard-Desce, M.; Fort, A.; Hu, Z.-Y.; Marder, S. R.; Perry, J. W.; Runser, C.; Staehelin, M.; Zysset, B. *Science* **1996**, *271*, 335.
(24) Akoudad, S.; Frère, P.; Mercier, N.; Roncali, J. *J. Org. Chem.* **1999**, *64*, 4267.
(25) Rawal, V. H.; Cava, M. P. *Chem. Commun.* **1984**, 1526.
(26) Willets, K. A.; Ostroverkhova, O.; He, M.; Twieg, R. J.; Moerner, W. E. *J. Am. Chem. Soc.* **2003**, *125*, 1174.
(27) Shenoy, V. U.; Patel, V. P.; Seshadri, S. *Dyes Pigm.* **1989**, *11*, 37.

(28) Cyclic voltammetry (CH_2Cl_2, 0.1 M [$^nBu_4N$][PF_6], 50 mV s^{-1}) shows EC-type processes (i.e., reversible electron transfer followed by chemical reaction on a comparable timescale) at +0.36 and −0.04 V vs $FeCp_2^{+/0}$ from **8** and **10**, respectively.

those of their thiophene analogues, also consistent with a greater ground-state charge transfer in the pyrrole chromophores, i.e., with the bis(pyrrole)ethylene core acting as a stronger π donor than bis(dialkoxythienyl)ethylene. Other evidence relating to ground-state charge transfer can be obtained from the $^1H-^1H$ NMR coupling constants associated with the protons of the vinylene π-bridges linking the heterocyclic (D) rings to the acceptor (A) groups. The values for the vinylene D—CH═CH—A bridges of **3** and **5** are 15.5 and 15.0 Hz indicating that (i) ground-state charge transfer is relatively limited in both cases, with neutral resonance structures predominating over charge-separated structures of the type D^+═CH—CH═A^- (coupling constants of ca. 16 or ca. 10 Hz expected for *trans* —CH═CH— and ═CH—CH═ entities, respectively,[29] with values of ca. 13.5 Hz found for species such as cyanine where the bond order is 1.5[30,31]) but that (ii) there is more contribution from charge-separated structures in the case of the chromophore with pyrrole donors. Consistent with the limited ground-state charge transfer implied by the coupling constants, there is considerable bond-length alternation (ca. 0.07 Å) in the AM1-calculated geometries of these polyene π-bridges in the sense implied by the neutral resonance structures shown in Figure 1, with a slightly (ca. 0.002 Å) longer CH═CH bond in the vinylene group linking donor and acceptor and a slightly shorter CH—A bond in **5** than in **3**. The D—CH bond is slightly longer for **5** than **3**, presumably for steric reasons (see discussion of geometry in calculation section below). Similar patterns are seen when comparing the calculated geometries of **6** and **7**. The AM1-calculated Mulliken partial charges on the bridge and acceptor portions of the molecule are also consistent with a larger charge separation in the pyrrole species than in their thiophene analogues (see the Supporting Information for details); however, the observed differences between, say, **6** and **7** are very small. To check that these small deviations are not an AM1-related artifact, we also calculated the Mulliken charges for density functional theory (DFT) optimized geometries (B3LYP/6-31*G); again, more charge separation is obtained for pyrrole-bridged species and, in fact, the trends are more pronounced than those seen in the AM1 results. The stronger donor character of pyrrole-based bridges can be understood in terms of their greater electron-richness, as evidenced, for example, by comparison of the $E_{1/2}^{+/0}$ for **8** and **10**.[28,32]

The TCF—CF_3 chromophores **3** and **4** are less readily oxidized than their respective TCF analogues (**1** and **2**) by 60—70 mV, consistent with more ground-state charge transfer in the former systems and with previous reports of the superior π-acceptor strength of TCF—CF_3.[33] Again, this trend is supported by the vinylene coupling constants (J = 16.0 and 15.5 Hz for **1** and **3**, respectively), by the calculated bond lengths, and by the calculated partial charges.

In assessing the strength of the SDS acceptor group, it is perhaps best to compare **7** to **1** and **3**, or **6** to **5**, since all five have the same number of double bonds between the donor groups and the dicyanovinylidene portion of the acceptor group; $E_{1/2}^{+/0}$ data generally suggest that there is less ground-state charge transfer in **6** and **7** than in their respective TCF or TCF—CF_3 analogues. In this particular comparison, however, no clear-cut trends can be discerned in the calculated bond-length or partial-charge data. The $E_{1/2}^{+/0}$ data show the expected effects of elongating the π-bridge between the donor and the acceptor groups (**1** vs **2**; **3** vs **4**), i.e., more facile oxidation in the compounds with more extensive conjugation, while $E_{1/2}^{0/-}$ is rather insensitive to chain length.

Finally, we note that, in the case of **1** and **3**, the oxidation potentials are +0.73 and +0.80 V, respectively, somewhat higher than that for the Ag^+/Ag couple in the same solvent ($E_{1/2}(Ag^+/Ag)$ = +0.65 V in CH_2Cl_2 but is considerably less oxidizing in other solvents, for example, $E_{1/2}(Ag^+/Ag)$ = +0.04 V in MeCN[34]). The chromophores may, therefore, be potentially useful in the two-photon-induced photodeposition of silver, which relies on the two-photon dye reducing silver ions by photoinduced electron transfer while being incapable of electron transfer to silver ions in the ground state.[19,35]

One- and Two-Photon Spectroscopy. The one-photon absorption (1PA) and degenerate two-photon absorption (2PA) spectra, obtained using the Z-scan technique,[36,37] are shown in Figure 3 plotted vs transition energy; the corresponding spectroscopic parameters are reported in Table 2. In Figure 4, the 1PA and Z-scan 2PA data are replotted for compound **2**, along with nondegenerate 2PA spectra obtained using the white-light-continuum (WLC) pump—probe method;[38] comparable plots for all seven chromophores are supplied in the Supporting Information. The 1PA maximum is shifted to a longer wavelength by 0.09—0.13 eV when the π-bridges between the donor and each acceptor group of **1** and **3** are extended with an additional double bond. The one-photon absorption maximum is also red-shifted (0.15—0.19 eV) when the TCF is replaced by the CF_3—TCF acceptor group. The maxima are red-shifted still further when the CF_3—TCF is replaced by SDS. Replacement of the 3,4-dibutoxylthiophene donors with *N*-hexylpyrrole groups also leads to a red shift (0.29—0.33 eV) in the maximum. In addition, in contrast to the broad featureless absorption profiles in the thiophene chromophores, their pyrrole analogues show narrower absorption profiles and poorly resolved

(29) Pretsch, E.; Bühlmann, P.; Affolter, C. *Structure Determination of Organic Compounds*. Springer-Verlag: Berlin, 2000.
(30) Tolbert, L. M.; Zhao, X. *J. Am. Chem. Soc.* **1997**, *119*, 3253.
(31) Barlow, S.; Henling, L. M.; Day, M. W.; Schaefer, W. P.; Green, J. C.; Hascall, T.; Marder, S. R. *J. Am. Chem. Soc.* **2002**, *124*, 6285.
(32) The ionization energies of pyrrole and thiophene are 8.9 and 8.2 eV, respectively (Sell, J. A.; Kuppermann, A. *Chem. Phys. Lett.* **1978**, *61*, 355), although a smaller difference might expected between pyrrole and dialkoxythiophene. The lower aromaticity of pyrrole (Katrinsky, A. R. *Handbook of Heterocyclic Chemistry*; Pergamon: Oxford, 1985) may also play a role in favoring a charge-separated structure.
(33) Liao, Y.; Eichinger, B. E.; Firestone, K. A.; Haller, M.; Luo, J.; Kaminsky, W.; Benedict, J. B.; Reid, P. J.; Jen, A. K.-Y.; Dalton, L. R.; Robinson, B. H. *J. Am. Chem. Soc.* **2005**, *127*, 2759.
(34) Connelly, N. G.; Geiger, W. E. *Chem. Rev.* **1996**, *96*, 877.
(35) Stellacci, F.; Bauer, C. A.; Meyer-Friedrichsen, T.; Wenseleers, W.; Alain, V.; Kuebler, S. M.; Pond, S. J. K.; Zhang, Y.; Marder, S. R.; Perry, J. W. *Adv. Mater.* **2002**, *14*, 194.
(36) Sheik-bahae, M.; Said, A. A.; Van Stryland, E. W. *Opt. Lett.* **1989**, *14*, 955.
(37) Sheik-bahae, M.; Said, A. A.; Wei, T.-H.; Hagan, D. J.; Van Stryland, E. W. *IEEE J. Quantum Electron.* **1990**, *26*, 760.
(38) Negres, R. A.; Hales, J. M.; Kobyakov, A.; Hagan, D. J.; Van, Stryland, E. W. *Opt. Lett.* **2002**, *27*, 270.

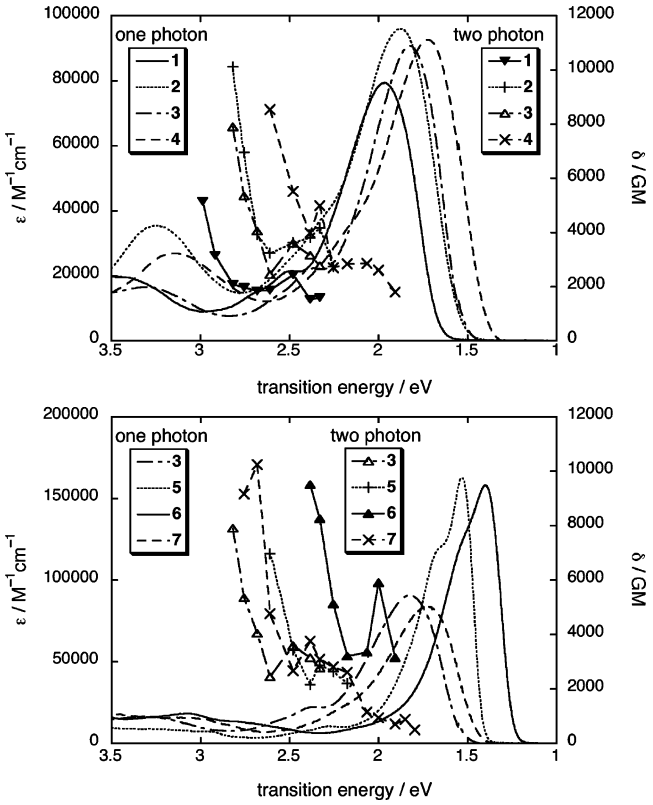

Figure 3. Two-photon spectra, acquired using Z-scan, and one-photon spectra for the following: **1**−**4** (above) allowing comparison of the effect of TCF vs TCF−CF_3 (**1** vs **3**; **2** vs **4**) and conjugation length (**1** vs **2**; **3** vs **4**); **3** and **5**−**7** (below) allowing comparison of TCF−CF_3 and SDS acceptors (**3** vs **7**; **5** vs **6**) and of pyrrole and dialkoxythiophene donors (**3** vs **5**; **6** vs **7**). All data were acquired in THF solution.

Table 2. Experimental One- and Two-Photon Absorption Parameters for 1−7

	1	**2**	**3**	**4**	**5**	**6**	**7**
$\lambda^{(1)}_{max}$ (nm)[a]	616	661	679	718	811	889	719
$E^{(1)}_{max}$ (eV)[b]	2.01	1.88	1.82	1.73	1.53	1.39	1.72
ϵ (M^{-1} cm^{-1})[a]	77 400	96 000	91 000	92 800	160 000	158 000	84 200
M_{ge} (D)[c]	13.7	15.8	14.9	16.3	17.4	19.2	14.5
$\lambda^{(2)}_{max}$ (nm)[d]	1000	1064	1000	1064	1064	1240	1040
$E^{(2)}_{max}$ (eV)[e]	2.48	2.33	2.48	2.33	2.33	2.00	2.38
δ_{max} (GM)[d]	2400	4200	3600	5000	2900	5900	3800

[a] Low-energy 1PA peak ($\lambda^{(1)}_{max}$), maximum molar extinction coefficient (ϵ_{max}). [b] Energy of the 1PA peak. [c] M_{ge}, transition dipole moment for the low-energy 1PA transition. [d] $\lambda^{(2)}_{max}$ and δ_{max} are the approximate photon wavelength for the low-energy two-photon peak and the corresponding cross section, respectively, according to Z-scan measurements (1 GM = 1×10^{-50} cm^4 s/photon). The error in the values of δ_{max} are estimated to be approximately ±20%. [e] $E^{(2)}$ (in eV) is the approximate total two-photon excitation energy (twice the photon energy at the given wavelength).

vibronic structure ($\Delta\nu = 1100-1200$ cm^{-1}); this narrowing of the absorption profile is reminiscent of changes seen as the ground-state transfer in donor−acceptor chromophores as one approaches the "cyanine limit" and is, therefore, perhaps related to the greater ground-state charge transfer present in the pyrrole systems (see the previous section).

The degenerate 2PA (Z-scan) spectra for all seven chromophores are similar in that they all show a poorly resolved low-energy peak with δ ranging from 2500 to 5900 GM (1 GM = 1×10^{-50} cm^4 s/photon) in the photon wavelength range $\lambda^{(2)}_{max} = 1.0-1.3$ μm (photon energy of 0.7−1.0 eV, transition energy of 1.4−2.0 eV). For the spectra extending to wavelengths significantly longer than those

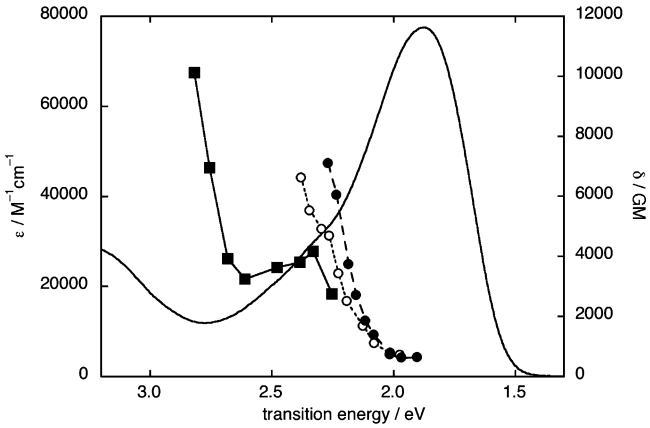

Figure 4. 1PA spectrum of **2** (solid line) compared with a degenerate 2PA spectrum from Z-scan measurements (solid squares, solid line) and with nondegenerate 2PA spectra acquired using the WLC with pump wavelengths of 1400 and 1600 nm (open circles, dotted line and solid circles, dashed line, respectively). All data were acquired in THF solution.

of this peak (spectra for **4** and **7**), one also sees indications of a weaker shoulder at photon wavelengths approaching twice that for 1PA, i.e., corresponding to 2PA into a state with an energy similar to that of the lowest lying 1PA state (vide infra). The cross sections for the peaks at 1.0−1.3 μm are of similar magnitude to those previously measured using the two-photon-induced fluorescence technique for bis-(styrylbenzene) chromophores with alkoxy groups imparting donor character to the bridge and SDS (4400 GM; structure shown in Figure 1, top left) or *N*,*N*-diethylthiobarbituric acid (1750 GM) acceptor end groups;[10] however, the transitions in the present chromophores are somewhat red-shifted relative to these previously studied compounds (for which $\lambda^{(2)}_{max} = 970-975$ nm).

The main low-energy feature, described above, appears as a shoulder of a much stronger absorption, whose peak lies at photon energies close to, or higher than, the energy of the 1PA absorption edge. As shown in Figures 2 and 3, the cross section measurable for the high-energy peak of **2** is ca. 10^4 GM; in all cases, the highest energy measurable values of δ are in excess of 5000 GM and large cross sections of greater than 2000 GM can be accessed over a transition-energy range of >0.5 eV, which corresponds to a photon-energy range of at least 0.25 eV.

2PA data were also acquired in the vicinity of the low-energy peak using the nondegenerate white-light-continuum (WLC) pump−probe method (use of this technique at high transition energies being precluded by 1PA of the probe beam). As shown in Figure 4, the WLC data afford larger cross sections than the Z-scan data; these cross sections increase as the wavelength difference between the pump and probe is increased, as expected from preresonance enhancement effects.[39] Moreover, as previously seen in other chromophores, the low-energy peak position is less well-defined for the nondegenerate measurements, which can also be rationalized by the increasing enhancement at shorter probe wavelengths.[27] Nevertheless, the WLC measurements confirm that **1**−**7** show strong 2PA in the NIR.

(39) Hales, J. M.; Hagan, D. J.; Van Stryland, E. W.; Schafer, K. J.; Morales, A. R.; Belfield, K. D.; Pacher, P.; Kwon, O.; Zojer, E.; Brédas, J. L. *J. Chem. Phys.* **2004**, *121*, 3152.

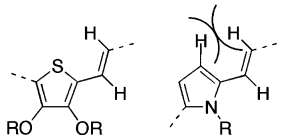

Figure 5. Schematic showing the steric origin of greater twist in the core of the pyrrole-based chromophores.

Comparing **1** to **2** and **3** to **4**, it can be seen that the extension of the π-bridges by one double bond results in both a lowering of the low-energy 2PA state energy (comparable to the shift in 1PA energy) and an increase in δ into that state by 40−70%. The CF_3−TCF chromophores **3** and **4** also show low-energy cross sections somewhat larger than their TCF analogues (**1** and **2**, respectively). On replacement of the 3,4-dialkoxythiophenes with the more strongly donating pyrrole groups, the energy of the 2PA state is lowered; the apparent cross section δ decreases from **3** to **5** but increases from **7** to **6**, although these changes are barely significant given the estimated experimental error in δ of ca. ±20%.

Quantum-Chemical Calculations. In order to gain more insight into the trends seen in the energy and strength of the electronic transitions upon chemical structure modification, quantum-chemical calculations were performed on **1**−**7** (with butyl and hexyl groups replaced by methyl groups to simplify the calculations). As discussed in the electrochemical section, the calculated variations among the chromophores in bond-length alternation in the D−CH=CH−A π-bridges are rather small. The calculated geometries of the π systems are essentially planar. The most significant deviations from planarity in the AM1-optimized structures are in the central D−CH=CH−D cores, with dihedral angles between the planes of the donor heterocycles and the planes of the central vinylene units of 1−10° for thiophene chromophores (**1**−**4** and **7**) and 12−19° for the pyrrole chromophores (**5** and **6**). The larger distortions in the pyrrole case can be attributed to steric interactions, as shown in Figure 5. The D−CH=CH−A portions of both pyrrole and thiophene chromophores are generally more planar than the cores; these portions of the pyrrole chromophores are slightly *more* planar than those of their thiophene analogues. The dihedral angles between the heterocycle and the vinylene bridges of **5** and **6** are 0−1° and 3−3.5°, respectively), while the corresponding angles for **3** and **7** are 2.5 and 6°, respectively, despite more steric crowding in the former pair of compounds. This is consistent with the increased ground-state charge transfer suggested in the pyrrole species by the electrochemical measurements (vide supra). DFT-optimized geometries, on the other hand, are consistently more planar (torsion angles < 3.2°) with no systematic variation between pyrrole and thiophene derivatives.

The MRDCI-calculated 1PA transition energies for the AM1-optimized structures are overestimated, in part due to overcorrelation of the ground state, as is typical for the method;[10] however, the trend fits the experimental trend reasonably well, except for the two pyrrole-containing compounds, **5** and **6**, for which the transition energies are more severely overestimated, regardless of whether the SCI or MRDCI schemes are used. While the INDO/MRDCI 1PA transition energies calculated at geometries obtained from DFT are smaller than those for the AM1 geometries (see the Supporting Information for values), the difference is not significant and compounds **5** and **6** still show the largest deviation from the experimental values. The following discussion is based on the results from the AM1 geometries, although very similar results are obtained using the DFT geometries.

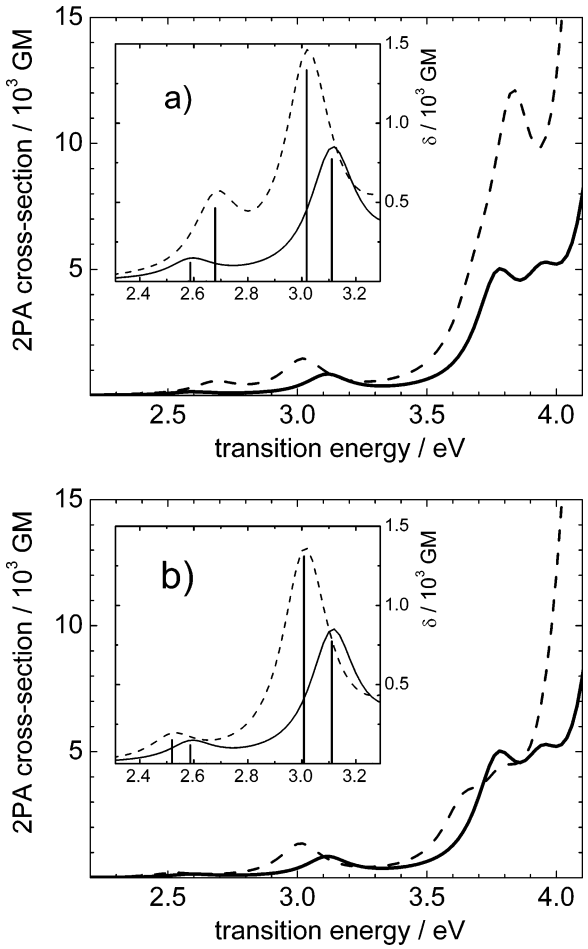

Figure 6. Comparison of the calculated 2PA spectra of compound **1** with those of (a) **2** and (b) **3** plotted vs transition (i.e., excited-state) energy. The profiles (**1** solid; **2** and **3** dashed lines) represent the 2PA cross section calculated from the SOS method. (inset) Low-energy portion of the spectra discussed in the text, along with vertical bars corresponding to 2PA cross sections calculated from the 2PA tensor.

The simulated 2PA spectra in Figure 6 are similar to the experimental spectra in that they consist of a low-energy (calculated transition-energy range of 2.0−3.4 eV) feature (or features) with δ of the order of 10^3 GM and a much stronger transition at higher energy (calculated at transition energies of 3.4−4.4. eV). The calculations indicate two significant 2PA transitions in the low-energy region for the thiophene-containing chromophores (Table 3). The lower energy of these two transitions has the smaller cross section for **1**−**4** but the higher cross section for **7**. This is consistent with the experimental observation of low-energy shoulders in **4** and **7** discussed above, although for **7** the intensity ratio for those peaks/shoulders appears to be reversed. This is, however, hard to quantify, as the experimentally stronger of the low-energy features sits as a shoulder on the much stronger high-energy maximum (see Figure 3).

Table 3. State Energies, E (eV), and Two-Photon Cross Sections, δ (GM), Calculated Using the INDO/MRDCI/2PA-tensor Method for the Lowest Energy Excited States of Chromophores 1−7

	S_1		S_2		S_3	
	E	δ	E	δ	E	δ
1	2.59	118	2.64	*a*	3.11	773
2	2.58	*a*	2.68	464	3.02	1334
3	2.52	150	2.55	*a*	3.01	1310
4	2.49	*a*	2.62	797	2.90	1881
5	2.44	*a*	2.75	2002		
6	2.25	*a*	2.53	3781		
7	2.21	*a*	2.46	2203	2.84	1489

[a] One-photon-allowed and two-photon-forbidden transition.

The calculations indicate that the lowest energy two-photon state for the thiophene compounds is, in fact, close to the first one-photon state; as listed in Table 3, for two of the chromophores (**1** and **3**), the two-photon state corresponds to S_1, whereas, in the other chromophores, S_1 is 1PA-allowed and 2PA-forbidden. Considering how close S_1 and S_2 are in energy for the thiophene-containing compounds, the limited wavelength range over which we have measured 2PA means that we may not necessarily observe 2PA into the lowest of the two low-energy 2PA states in every experimental spectrum. For the pyrrole-containing chromophores, only one low-energy 2PA transition is calculated and the relevant state (S_2) lies significantly above the 1PA state. As with the 1PA maxima, the absolute transition energies are systematically overestimated by the MRDCI calculations; however, the trends are reasonably well-reproduced when one considers the limited number of experimental data points and, hence, limited resolution in determining the experimental 2PA maxima.

The calculated δ into S_3 (thiophene chromophores) or S_2 (pyrrole chromophores) increases on extending the π-bridge from **1** to **2** and from **3** to **4** and also as the strength of the acceptor group increases from **1** to **3** and from **2** to **4**. In addition, replacement of the TCF−CF_3 acceptor with the SDS acceptor leads to increased 2PA cross sections (**7** vs **3**; **6** vs **5**). The pyrrole-containing chromophores (**5** and **6**) are calculated to give higher δ values than their thiophene analogues, which is consistent with experimental results in the case of **6** vs **7**, but not in the case of **5** vs **3** (although the experimental differences between these are barely significant, given the experimental uncertainties). In general, the calculated cross sections (for the chosen broadening, which appears consistent with the experimental peak widths) are about a factor of 2 smaller than those measured by Z-scan. The magnitude of the latter is, however, affected by the stronger overlap with the high-energy 2PA features. A reason for the smaller calculated cross sections arises from the overestimated state energies. If experimental 1PA and 2PA transition energies from Table 2 are considered rather than the calculated energies, the δ values derived from the approximate 3-state model for quadrupolar molecules (vide infra) increase by a factor of about 1.3−2.2 due to reduced detuning factors, $(E_{ge} - E_{ge'}/2)^2$, despite also reduced $E_{ge'}{}^2$ terms, in eq 1 (vide infra).

In order to gain further insight into structure−property relationships, essential-state models have proven helpful. For degenerate 2PA in centrosymmetric systems, δ is typically approximated by[40]

$$\delta \propto \frac{M_{ge}{}^2 M_{ee'}{}^2}{(E_{ge} - E_{ge'}/2)^2} \times \left(\frac{E_{ge'}}{2}\right)^2 \qquad (1)$$

where M_{ge} is the transition dipole moment between the ground state g and the dominant one-photon-allowed excited state e, $M_{ee'}$ is the transition dipole moment between the 1PA and the 2PA states, and $E_{ge} - E_{ge'}/2$ is the so-called detuning energy. By calculating the 2PA cross section for the $S_0 \rightarrow S_3$ transition as a function of the number of intermediate excited states, one finds that 2PA into S_3 excitation for **1**−**4** and **7** can be reasonably well-described using a single three-state term; only the S_1 (**1** and **3**) or S_2 (**2**, **4**, and **7**) 1PA-allowed intermediate states need to be considered. Although higher-lying excited states also contribute to δ into S_3, as illustrated in Figure 7 for **4** as a representative example, these additional contributions essentially compensate each other. In contrast, 2PA into the S_1 state of **1** and **3** or into the S_2 state of **2**, **4** (Figure 6), and **7** requires a more complex description with several intermediate (higher-lying) excited states contributing more significantly to δ. Adequate description of 2PA into the S_2 state of **5** and **6** also requires consideration of multiple intermediate states.

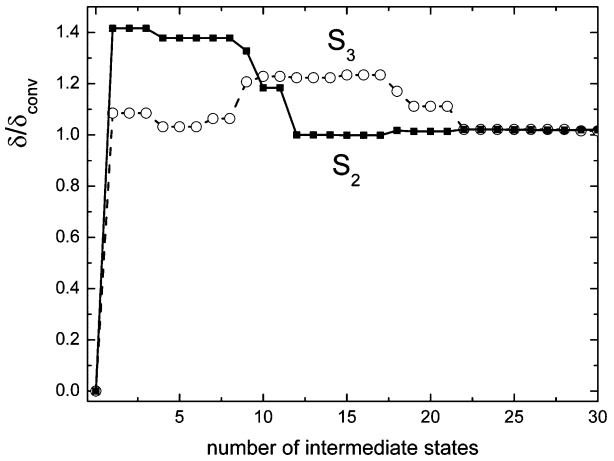

Figure 7. Calculated ratio δ/δ_{conv} (2PA-tensor values) for 2PA into S_2 and S_3 of chromophore **4** as a function of the number of intermediate excited states included (δ_{conv} denotes the fully converged cross section).

This implies that, at least, for 2PA into the S_3 states of **1**−**4** and **7**, the three-state expression (eq 1) allows an analysis of the observed trends in δ on the basis of the transition dipoles and excited-state energies. The corresponding quantities are given in Table 4. It can be seen that the increase in δ seen comparing chromophores with TCF and CF_3−TCF (i.e., when going from **1** to **3** and from **2** to **4**, respectively) is largely due to an increased coupling between the 1PA and the 2PA active states (i.e., an increase in $M_{ee'}$). Increasing the length of the conjugated backbone (i.e., **1** vs **2**; **3** vs **4**) results in a comparable increase of M_{ge} and $M_{ee'}$. In the chromophores discussed thus far (**1**−**4**), changes in the detuning energy play practically no role. The situation is significantly different in **7**, where the significantly decreased

(40) Albota, M.; Beljonne, D.; Brédas, J. L.; Ehrlich, J. E.; Fu, J.-Y.; Heikal, A. A.; Hess, S. E.; Kogej, T.; Levin, M. D.; Marder, S. R.; McCord-Maughon, D.; Perry, J. W.; Röckel, H.; Rumi, M.; Subramanian, G.; Webb, W. W.; Wu, X.-L.; Xu, C. *Science* **1998**, *281*, 1653.

Table 4. Quantities Entering the Three-State Expression for 2PA into the S_3 (e') State of 1−4 and 7 and into the S_2 (e') State of 5 and 6 Where e Denotes the S_1 (2, 4−7) or S_2 (1, 3) Intermediate 1PA-Allowed State

	1	2	3	4	5	6	7
E_{ge} (eV)	2.64	2.58	2.55	2.49	2.44	2.25	2.21
$E_{ge'}$ (eV)	3.11	3.02	3.01	2.90	2.75	2.53	2.84
$E_{ge} - E_{ge'}/2$ (eV)	1.09	1.07	1.05	1.04	1.07	0.99	0.79
M_{ge} (D)	13.5	15.3	13.9	15.7	15.8	15.9	14.6
$M_{ee'}$ (D)	10.1	12.2	12.9	14.1	16.9	24.5	10.8
$\delta_{3-state}$[a] (GM)	793	1454	1384	1996	2467	5192	1683

[a] Two-photon cross section obtained by the insertion of the above terms into eq 1. Converged values of δ are shown in Table 3.

detuning energy approximately compensates for the decrease in $M_{ee'}$ relative to the values for **2**, **3**, and **4**, resulting in comparable cross sections for all four chromophores. Here, **7** also shows the smallest experimental detuning energy, although the trend inferred from experiment is less pronounced.

Conclusion

Quadrupolar A−D−A type molecules with strong acceptors (TCF, CF_3−TCF, and SDS) and electron-rich bis(heterocycle)ethylene donors (heterocycle = dialkoxythiophene, pyrrole) have been synthesized. All chromophores show strong 2PA absorption (cross sections, δ, of 2400−5900 GM) in the 1.0−1.3 μm photon wavelength range, with even higher δ (from 5200 to 10100 GM) accessible at higher energies due to the onset of a much stronger peak. For each compound, 2PA cross sections of over 2000 GM can be accessed in a photon-energy range of over 0.25 eV (i.e., transition energy range of >0.5 eV). The trends observed in the energies and cross sections of the low-energy 2PA features can be correlated to features of the chemical structures and are generally well-reproduced using ZINDO/MRCDI calculations. The observed 2PA absorptions in the near-IR can be attributed to absorption into the S_3 and S_2 states for thiophene-based and pyrrole-based chromophores, respectively. In the former class of compounds, the absorption into S_3 can be well-described by a single three-state expression where the lowest-energy one-photon state is the only significant intermediate state. Some of these chromophores may be useful for 3D fabrication by 2PA-induced photodeposition of silver.

Experimental

***E*-1,2-Bis(5-vinylformyl-3,4-dibutoxy-2-thienyl)ethylene (9)**. To a solution of 1,2-bis(3,4-dibutoxy-2-thiophenyl)ethylene,[24] **8** (1.43 g, 2.97 mmol), in THF (50 mL), ^{n}BuLi (2.5 mL, 6.24 mmol, 2.5 M in hexane) at 0 °C was added. After the solution was stirred at 0 °C for 1 h, 3-(dimethylamino)propenal (0.516 g, 3.0 mmol) was added at 0 °C. The mixture was stirred at room temperature for 2 h. The mixture was worked up with 0.5 N HCl aqueous solution and extracted with diethyl ether. Column chromatography (silica gel, dichloromethane, and then ethyl acetate) gave a red solid (0.80 g, 47%). ^{1}H NMR ($CDCl_3$, 500 MHz) δ 9.58 (d, J = 7.8 Hz, 2H), 7.56 (d, J = 15.6 Hz, 2H), 7.04 (s, 2H), 6.37 (dd, J = 15.6, 7.8 Hz, 2H), 4.15 (t, J = 6.7 Hz, 4H), 4.03 (t, J = 6.6 Hz, 4H), 1.74 (m, 8H), 1.50 (m, 8H), 0.98 (m, 12H). Anal calcd for $C_{32}H_{44}O_6S_2$: C, 65.27; H, 7.53. Found: C, 65.40; H, 7.66.

1-Hexyl-1*H*-pyrrole-2-carbaldehyde. A solution of pyrrole-2-carbaldehyde (6.800 g, 71.50 mmol) in anhydrous DMF (20 mL) was added dropwise at 0 °C under nitrogen to a suspension of NaH (3.200 g of a 60% suspension in mineral oil, 80.00 mmol) in the same solvent (20 mL). The resulting white suspension was stirred at 0 °C for 30 min. A solution of *n*-hexylbromide (12.440 g, 75.00 mmol) in anhydrous DMF (30 mL) was added dropwise observing evolution of a colorless gas. The gray suspension was stirred at room temperature for 3 d and then poured into ice-cold water (300 mL) and extracted with Et_2O (2 × 200 mL). The organic phase was washed with water (5 × 100 mL), dried over $MgSO_4$, and evaporated at reduced pressure yielding the title compound as a yellow oil (12.50 g, 69.8 mmol, yield 98%). ^{1}H NMR ($CDCl_3$) δ 9.52 (s, 1H), 6.92 (m, 2H), 6.20 (m, 1H), 4.29 (t, J = 7.2 Hz, 2H), 3.47 (q, J = 7.2 Hz, 2H), 1.73 (quint broad, J = 6.0 Hz, 2H), 1.27 (m broad, 4H), 0.86 (m broad, 3H). ^{13}C NMR ($CDCl_3$) δ 179.3, 131.4, 124.9, 109.6, 66.1, 49.5, 31.7, 26.5, 22.9, 15.7. MS (EI, T = 41 °C) m/z (%) 179 (65)[M^+], 150 (100), 136 (17), 108 (40), 94 (34), 80 (42).

***E*-1,2-Bis(1-hexyl-1*H*-pyrrol-2-yl)ethylene (10).** Zn (14.620 g, 223.60 mmol) was suspended under nitrogen in anhydrous THF (300 mL), and the suspension was cooled to −20 °C. $TiCl_4$ (21.210 g, 12.26 mL, 111.80 mmol) was added dropwise; the addition was accompanied by the formation of a yellow precipitate. The suspension was refluxed for 30 min and gradually darkened. The mixture was cooled to −15 °C, and a solution of 1-hexyl-1*H*-pyrrole-2-carbaldehyde (10.000 g, 55.90 mmol) and anhydrous pyridine (11.500 g, 145.34 mmol) in anhydrous THF (50 mL) was added dropwise. The resulting suspension was refluxed for 2 h and then poured into a 3:2 mixture of water and CH_2Cl_2 (600 mL). The dark suspension was filtered through a pad of Celite. The organic phase was separated and washed with water (3 × 200 mL), dried over $MgSO_4$, and concentrated yielding a yellow-green oil that was purified by flash chromatography (silica, CH_2Cl_2/hexane 9:1), affording the title compound as a bright yellow oil. (5.00 g, 15.34 mmol, yield 55%). ^{1}H NMR (CD_2Cl_2) δ 6.72 (s, 2H), 6.65 (dd, J^1 = 1.5 Hz, J^2 = 3.0 Hz, 2H), 6.38 (dd, J^1 = 3.6 Hz, J^2 = 1.80 Hz, 2H), 6.10 (dd, J^1 = 3.6 Hz, J^2 = 2.7 Hz, 2H), 3.93 (t, J = 7.8 Hz, 4H), 1.73 (quint, J = 7.2 Hz, 4H), 1.31 (m broad, 4H), 0.89 (t, J = 8.7 Hz, 6H). ^{13}C NMR (CD_2Cl_2) δ 131.80, 122.09, 114.83, 108.07, 105.49, 42.27, 31.97, 31.79, 26.81, 22.96, 14.15. MS (EI, T = 41 °C) m/z (%) 326 (100)[M^+], 255 (10), 241 (8), 171 (14), 118 (5), 55 (6), 42 (15). Anal calcd for $C_{22}H_{34}N_2$: C, 80.93; H, 10.50; N, 8.58. Found: C, 80.80; H, 10.41; N, 8.44.

***E*-1,2-Bis(5-vinylformyl-*N*-hexyl-2-pyrrolyl)ethylene (11).** 3-(Dimethylamino)propenal (1.490 g, 15.00 mmol), was added dropwise under nitrogen to freshly distilled $POCl_3$ (2.300 g, 15.00 mmol). The resulting red viscous oil was taken up with anhydrous acetonitrile (20 mL), and the resulting red solution was stirred at 0 °C for 30 min. A solution of *E*-1,2-bis(*N*-hexyl-2-pyrrolyl)-ethylene, **10** (1.500 g, 4.59 mmol), in anhydrous acetonitrile (30 mL) was added dropwise and the resulting deep blue solution was stirred overnight at room temperature. The solution was poured into 10% aqueous NaOAc (300 mL) and stirred for 30 min at room temperature. K_2CO_3 (20 g) was added and organic phase turned red; the mixture was diluted with ethyl acetate (150 mL) and phases were separated. The organic phase was washed with brine (100 mL), dried over $MgSO_4$ and evaporated, affording a red residue that was taken up with MeOH and filtered. Crystallization (MeOH) of the precipitate afforded the pure title compound as a dark solid (0.750 g, 38%). ^{1}H NMR ($CDCl_3$, 300 MHz) δ 9.56 (d, J = 7.8 Hz, 2H), 7.33 (d, J = 15.3 Hz, 2H), 6.93 (s, 2H), 6.87 (d, J = 4.2 Hz, 2H), 6.67 (d, J = 4.2 Hz, 2H), 6.48 (dd, J = 15.3, 7.8 Hz, 2H), 4.10 (t, J = 7.5 Hz, 4H), 1.73 (quintet, J = 6.9 Hz, 4H),

1.43−1.24 (m, 12H), 0.89 (t, $J = 6.9$ Hz, 6H). ^{13}C NMR ($CDCl_3$, 75 MHz) δ 192.3, 138.8, 137.9, 130.5, 123.8, 116.7, 114.6, 109.3, 43.8, 31.9, 31.7, 26.7, 22.9, 14.1. MS (EI) *m*/*z* (%) 434.3 (100), 405.3 (4), 380.3 (5). Anal calcd for $C_{28}H_{38}N_2O_2$: C, 77.38; H, 8.81; N, 6.45. Found: C, 77.14; H, 8.83; N, 6.63.

***E*-1,2-Bis(5-formyl-*N*-hexyl-2-pyrrolyl)ethylene (13).** Anhydrous DMF (1.111 g, 15.20 mmol) was added dropwise under nitrogen and at 0 °C to freshly distilled $POCl_3$ (2.330 g,15.20 mmol), and the resulting viscous solution was stirred until completely converted into a glassy white solid that was taken up with anhydrous CH_3CN (15 mL). The resulting pale yellow solution was added dropwise, again at 0 °C, to a solution of **10** (2.040 g, 6.25 mmol) in anhydrous CH_3CN (30 mL); the solution turned red. After 2 h at room temperature, the solution was poured into 10% aqueous NaOAc (500 mL), neutralized with solid K_2CO_3, and extracted with ethyl acetate (150 mL). The organic layer was washed with water (2 × 100 mL), dried over Na_2SO_4, and evaporated, yielding a brown oil (2.300 g). Chromatographic separation afforded the title compound as a bright yellow solid. (1.130 g, 2.94 mmol, yield 47.3%). ^{1}H NMR ($CDCl_3$) δ 9.50 (s, 1H), 6.98 (s, 2H), 6.94 (d, $J = 4.5$ Hz, 2H), 6.58 (d, $J = 4.5$ Hz, 2H), 4.44 (t, $J = 6.9$ Hz, 4H), 1.72 (quint, $J = 6.9$ Hz, 4H), 1.31 (m broad, 4H), 0.87 (t, $J = 6.6$ Hz, 6H). ^{13}C NMR ($CDCl_3$) δ 178.8, 141.1, 132.7, 125.2, 118.9, 108.6, 45.5, 31.8, 30.1, 26.7, 22.9, 14.4. MS (EI, $T = 130$ °C) *m*/*z* (%) 382 (100) [M^+], 354 (21), 326 (5), 311 (4), 283 (4), 255 (5), 190 (4), 169 (4), 156 (1). Anal calcd for $C_{24}H_{34}N_2O_2$: C, 75.35; H, 8.96; N, 7.32. Found: C, 75.41; H, 8.98; N, 7.23.

Compound 1. A mixture of **12**[24] (0.200 g, 0.37 mmol) and TCF acceptor (0.243 g, 1.22 mmol) in ethanol (1.0 mL) was heated in a CEM Discover Labmate microwave reactor at 80 W and 100 °C for 1 h. After cooling down to room temperature, filtration and washing with ethanol gave a dark green crystalline solid (0.22 g, 67%). ^{1}H NMR ($CDCl_3$, 400 MHz) δ 7.80 (d, $J = 16.0$ Hz, 2H), 7.15 (s, 2H), 6.60 (d, $J = 15.9$ Hz, 2H), 4.25 (t, $J = 6.6$ Hz, 4H), 4.06 (t, $J = 6.7$ Hz, 4H), 1.76 (m, 8H), 1.73 (s, 12H), 1.48 (m, 8H), 0.99 (m, 12H). ^{13}C NMR ($CDCl_3$, 100 MHz) δ 175.49, 172.92, 154.94, 148.76, 135.34, 134.07, 122.46, 119.81, 112.04, 111.29, 111.22, 110.78, 97.18, 96.89, 74.81, 74.15, 56.56, 32.04, 31.91, 26.63, 19.12, 13.86, 13.78. UV−vis (THF) λ 631 nm (80 000 M^{-1} cm^{-1}). MS (MALDI) *m*/*z* 898 (M^+). Anal calcd for $C_{50}H_{54}N_6O_6S_2$: C, 66.79; H, 6.05; N, 9.35. Found: C, 66.80; H, 5.93; N, 9.35.

Compound 2. A mixture of compound **9** (0.252 g, 0,43 mmol) and TCF acceptor (0.342 g, 1.72 mmol) in ethanol (1 mL) was heated with a CEM Discover Labmate microwave reactor at 80 W and 100 °C under nitrogen for 1 h. After cooling down to room temperature, filtration gave a black solid, which was purified by recrystallization in ethanol (4 mL) to afford compound **2** as a black solid (0.233 g, 57%). ^{1}H NMR ($CDCl_3$, 400 MHz) δ 7.50 (dd, $J =$ 11.1, 15.2 Hz, 2H), 7.26 (d, $J = 15.2$ Hz, 2H), 7.06 (s, 2H), 6.69 (dd, $J = 11.2$, 14.8 Hz, 2H), 6.42 (d, $J = 15.3$ Hz, 2H), 4.16 (t, J $= 6.6$ Hz, 4H), 4.05 (t, $J = 6.6$ Hz, 4H), 1.75 (m, 8H), 1.70 (s, 12H), 1.49 (m, 8H), 0.99 (m, 12H). ^{13}C NMR ($CDCl_3$, 100 MHz) δ 175.63, 172.79, 152.49, 148.59, 147.63, 134.82, 130.99, 125.27, 123.50, 118.68, 117.03, 112.09, 111.30, 110.96, 97.00, 96.84, 74.37, 74.01, 56.52, 32.01, 31.97, 26.46, 19.13, 19.07, 13.90, 13.84. UV−vis (THF) λ 661 nm (96 000 M^{-1} cm^{-1}). Anal calcd for $C_{54}H_{58}N_6O_6S_2$: C, 68.18; H, 6.15; N, 8.84. Found: C, 68.15; H, 6.17; N, 8.83.

Compound 3. A mixture of **12** (0.233 g, 0.43 mmol) and CF_3−TCF (0.324 g, 1.28 mmol) in ethanol (2 mL) was heated at 20 W and 100 °C for 20 min in a CEM Discover Labmate microwave reactor. Filtration and washing with methanol gave a dark green solid as crude product (0.37 g), which was recrystallized from ethanol to give a green solid (0.347 g, 80%). ^{1}H NMR ($CDCl_3$, 500 MHz) δ 8.21 (d, $J = 15.6$ Hz, 2H), 7.21 (s, 2H), 6.56 (d, $J =$ 15.6 Hz, 2H), 4.28 (m, 4H), 4.07 (m, 4H), 1.91 (s, 6H), 1.76 (m, 8H), 1.47 (m, 8H), 0.99 (t, $J = 7.3$ Hz, 6H), 0.96 (t, $J = 7.4$ Hz, 6H). ^{13}C NMR ($CDCl_3$, 125 MHz) δ 174.83, 162.40, 156.33, 149.08, 137.54, 135.94, 123.14, 120.63, 110.77, 110.64, 110.37, 110.25, 97.88, 93.63, 74.96, 74.52, 59.16, 32.00, 31.90, 19.27, 19.12, 18.98, 13.83, 13.73. UV−vis (THF) λ_{max} 670 nm (91 000 M^{-1} cm^{-1}). HRMS (MALDI) calcd for $C_{50}H_{48}F_6N_6O_6S_2$: 1006.2981. Found: 1006.3075. Anal calcd for $C_{50}H_{48}F_6N_6O_6S_2$: C, 59.63; H, 4.80; N, 8.34. Found: C, 59.74; H, 4.85; N, 8.14.

Compound 4. A mixture of compound **9** (0.235 g, 0.40 mmol) and CF_3−TCF (0.253 g, 1.0 mmol) in ethanol is heated with a CEM Discover Labmate microwave reactor at 10 W and 90 °C for 10 min. After the reaction mixture was allowed to cool, filtration gave a brown crystalline solid as the crude product (0.36 g, 83%). The crude product was purified by column chromatography (silica gel, dichloromethane, and then dichloromethane/ethyl acetate 10:1) and gave a brown solid (0.30 g, 71%). ^{1}H NMR ($CDCl_3$, 500 MHz) δ 7.89 (dd, $J = 11.4$, 14.8 Hz, 2H), 7.37 (d, $J = 14.7$ Hz, 2H), 7.10 (s, 2H), 6.72 (dd, $J = 11.4$, 14.7 Hz, 2H), 6.36 (d, $J = 15.0$ Hz, 2H), 4.19 (t, $J = 6.7$ Hz, 4H), 4.05 (t, $J = 6.6$ Hz, 4H), 1.87 (s, 6H), 1.76 (m, 8H), 1.49 (m, 8H), 1.00 (t, $J = 7.3$ Hz, 6H), 0.98 (t, $J = 7.5$ Hz, 6H). ^{13}C NMR ($CDCl_3$, 125 MHz) δ 174.98, 162.03, 153.57, 150.03, 148.88, 137.00, 132.65, 125.78, 124.08, 119.31, 116.04, 110.88, 110.84, 110.29, 97.36, 93.57, 74.48, 74.13, 59.00, 31.97, 31.95, 19.11 (double intensity), 19.04, 13.88, 13.79. UV−vis (THF) λ_{max} 718 nm (92 800 M^{-1} cm^{-1}). HRMS (MALDI) calcd for $C_{54}H_{52}F_6N_6O_6S_2$: 1058.3294. Found: 1058.3257. Anal calcd for $C_{54}H_{52}F_6N_6O_6S_2$: C, 61.24; H, 4.95; N, 7.93. Found: C, 61.37; H, 5.02; N, 7.78.

Compound 5. A suspension of **13** (0.15 g, 0.39 mmol) and CF_3−TCF (0.202 g, 0.80 mmol) in ethanol (3 mL) was placed in a 10 mL sealed vessel and heated under CEM Discover Labmate microwave irradiation at a constant power of 50 W for 30 min and at a constant power of 90 W for 30 min. The resulting deep blue suspension was cooled and filtered affording a green shiny powder that was washed directly on the filter with ethanol (15 mL) (0.27 g, 81% yield). ^{1}H NMR (acetone-d_6, 300 MHz) δ 8.45 (d, $J =$ 15.0 Hz, 2H), 7.78−7.69 (m broad, 4 H), 7.39 (d broad, $J = 4.5$ Hz, 2H), 6.98 (d, $J = 14.7$ Hz, 2H), 4.44 (t broad, 4H), 2.80 (m broad, 4H), 1.48−1.22 (m broad, 12H), 0.85 (t broad, 6H). ^{1}H NMR (CD_2Cl_2, 75 MHz) δ 8.30 (d, $J = 14.6$ Hz, 2H), 7.33 (d, $J = 4.9$ Hz, 2H), 7.14 (s, 2H), 7.02 (d, $J = 4.6$ Hz, 2H), 6.56 (d, $J = 15.0$ Hz, 2 H), 4.16 (t, $J = 8.0$ Hz, 4H), 1.84−1.73 (m, 4H), 1.56 (s, 6H), 1.45−1.23 (m, 12H), 0.93−0.85 (m, 6H). MS (FAB) *m*/*z* (relative intensity) 853 (100), 804 (7), 665 (3). Anal calcd for $C_{46}H_{42}F_6N_8O_2$: C, 64.78; H, 4.96; N, 13.14. Found: C, 64.69; H, 4.97; N, 13.11.

Compound 6. A suspension of dialdehyde **11** (0.215 g, 0.49 mmol) and 3-dicyanomethylidene-2,3-dihydrobenzothiophene-1,1-dioxide (0.250, 1.09 mmol) in ethanol (6 mL) was placed in a 10 mL sealed vial and heated under CEM Discover Labmate microwave irradiation at a constant power of 50 W for 10 min and at a constant temperature of 130 °C for 3 min. The resulting dark solution was cooled at 0 °C and filtered affording a golden-brown precipitate that was washed with a copious amount of ethanol and dried. (0.32 g, 76% yield). ^{1}H NMR (CD_2Cl_2, 300 MHz) δ 8.85−8.81 (m, 2H), 8.53 (d, $J = 12.7$ Hz, 2H), 7.96 (dd, $J = 7.5$, 2.7 Hz, 2H), 7.86 (td, $J = 7.5$, 2.1 Hz, 2H), 7.83 (td, $J = 7.3$, 2.0 Hz, 2H), 7.61 (d, $J = 13.8$ Hz, 2H), 7.57 (d, $J = 13.6$ Hz, 2H), 7.25 (d, $J =$ 4.9 Hz, 2H), 7.24 (d, $J = 13.1$ Hz, 2H), 7.10 (s, 2H), 6.96 (d, $J =$ 4.7 Hz, 2H), 4.17 (t, $J = 7.9$ Hz, 4H), 1.83−1.68 (m, 4H), 1.59−1.24 (m, 12H), 0.95−0.85 (m, 6H). MS (FAB) *m*/*z* (relative intensity) 859 (6), 810 (3), 766 (4), 596 (6), 443 (18), 341 (13).

Anal calcd for $C_{50}H_{46}N_6O_4S_2$: C, 69.91; H, 5.40; N, 9.78. Found: C, 69.65; H, 5.42; N, 9.59.

Compound 7. A mixture of 3-dicyanomethylidene-2,3-dihydrobenzothiophene-1,1-dioxide (343 mg, 1.5 mmol) and dialdehyde **9** (0.22 g, 0.37 mmol) in ethanol (5 mL) was heated with a CEM Discover Labmate microwave reactor at 85 °C and 50 W for 50 min. After cooling, filtration gave a dark brown green solid, which was purified by column chromatography (silica, dichloromethane, and then dichloromethane/ethyl acetate 10:1) to give a crude product as a dark brown solid (400 mg). The crude product was further purified by recrystallization (ethanol) and then column chromatography (silica, dichloromethane/ethyl acetate 20:1) to give a dark brown solid (0.16 g, 43%). ^{1}H NMR ($CDCl_3$, 500 MHz) δ 8.85 (d, $J = 7.4$ Hz, 2H), 8.50 (d, $J = 11.6$ Hz, 2H), 7.97 (dd, $J = 7.7$, 1.4 Hz, 2H), 7.82 (m, 4H), 7.55 (m, 4H), 7.19 (s, 2H), 4.26 (t, $J = 6.8$ Hz, 4H), 4.08 (t, $J = 6.7$ Hz, 4H), 1.81 (quintet, $J = 6.8$ Hz, 8H), 1.51 (m, 8H), 1.03 (t, $J = 7.4$ Hz, 6H), 0.98 (t, $J = 7.5$ Hz, 6H). ^{13}C NMR ($CDCl_3$, 100 MHz) δ 154.85, 149.23, 149.02, 143.47, 141.19, 138.60, 135.16, 134.95, 134.51, 128.99, 128.24, 125.92, 124.06, 122.04, 120.02, 119.93, 114.77, 114.70, 74.82, 74.17, 70.05, 31.94, 31.91, 19.16, 19.06, 13.90, 13.81. HRMS (MALDI) calcd for $C_{54}H_{52}N_4O_8S_4$: 1012.2668. Found: 1012.271. Anal calcd for $C_{54}H_{52}N_4O_8S_4$: C, 64.01; H, 5.17; N, 5.53. Found: C, 64.03; H, 5.28; N, 5.24.

Two-Photon Spectroscopy. The femtosecond laser source is a Ti:sapphire regenerative amplification system (CPA2010, CLARK-MXR), which provides laser pulses at 775 nm with 140 fs duration (full width half-maximum (fwhm)) at a 1 kHz repetition rate. This laser pumps two optical parametric amplifier (OPA) systems (TOPAS, Light Conversion), which can be tuned from 525−2200 nm (0.56−2.36 eV) and provide up to 100 μJ of energy. The degenerate 2PA spectra of the samples were measured by the single-wavelength Z-scan technique.[36,37] We use one of the OPAs to tune the wavelength and attenuate the output energy to 10−300 nJ for Z-scan measurement. Nondegenerate 2PA spectra were obtained using the femtosecond white-light-continuum (WLC) pump−probe nonlinear spectrometer method.[38] In this experimental setup, one OPA provides a strong pump beam whose irradiance can be up to 90 GW cm^{-2}. A 1300 nm beam of approximately 2 μJ of energy from the other identical OPA is focused into a 2.5 mm thick piece of calcium fluoride to generate a weak, broadband WLC probe (400−1500 nm, 0.83−3.1 eV). The nondegenerate 2PA process requires simultaneous absorption of one photon from both the pump and probe beams. Due to the temporal chirp nature of the generated WLC probe, we have to vary the temporal delay between the pump pulse and the WLC probe in order to obtain the entire 2PA spectra. Combined with a correction factor to account for the temporal walk-off between the pump and probe in the sample, we can characterize a sample's nondegenerate 2PA spectrum.

Quantum-Chemical Calculations. The geometries of chromophores **1**−**7** were optimized using the semiempirical Austin Model 1 (AM1)[41] method implemented in the AMPAC 8 package.[42] On the basis of the AM1-optimized geometries, the electronic properties (state dipole moments, transition dipole moments, and transition energies) were evaluated from the semiempirical intermediate neglect of differential overlap (INDO) Hamiltonian.[43] The spectroscopic parametrization along with the Mataga−Nishimoto electron repulsion scheme[44] was used, as implemented in the ZINDO code.[45,46] For consistency with previous calculations, the original INDO/S parametrization[47] was used throughout; readers should be aware that the default parameter set for our ZINDO implementation differs somewhat from the original (e.g., in the resonance integral β for O). The INDO calculations were coupled to a multireference-determinants configuration-interaction (MRDCI) scheme.[48−50] The 10 highest occupied and 10 lowest unoccupied molecular orbitals were active in the MRDCI procedure for single and double excitations relative to the reference determinants. The SCF determinant, three singly excited determinants (HOMO → LUMO, HOMO − 1 → LUMO, HOMO → LUMO + 1), and the doubly excited determinant with both electrons promoted from the HOMO to the LUMO (HOMO,HOMO → LUMO,LUMO) were chosen as reference determinants. 2PA cross sections δ were calculated with the SOS expression[51] (using a uniform damping of $\Gamma = 0.1$ eV) and with the 2PA tensor[52−54] which both include the electronic parameters determined with INDO/MRDCI. To be consistent with the SOS calculations, the 2PA values reported (with respect to photon energies) for the tensor calculations correspond to the maxima of Lorentzian lineshapes with a fwhm of 0.1 eV when plotting the 2PA spectra as a function of photon energies (i.e., 0.2 eV in plots vs transition energy). Solvent effects have neither been included in the quantum-chemical simulations nor in the calculation of the 2PA cross sections. The geometries were also optimized at the DFT level using the 6-31G** basis set and the B3LYP functional as implemented in the Gaussian 03 program.[55]

Acknowledgment. This material is based upon work supported in part by the National Science Foundation through the STC Program under Agreement Number DMR-0120967 and through CRIF 04-43564. We also thank the Defense Advanced Research Projects Agency for funding through the MORPH program. The work done at CREOL was also supported by AFOSR under contract FA95500410200. We thank Greg Walker for preparing the SDS acceptor. L.A.P. thanks CAPES and FAPESP for financial support. ZS acknowledges the National

(41) Dewar, M. J. S.; Zoebisch, E. G.; Healy, E. F.; Stewart, J. J. P. *J. Am. Chem. Soc.* **1985**, *107*, 3902.
(42) *AMPAC 8*; Semichem, Inc.: P.O. Box 1649, Shawnee, KS 66222, copyright 1992−2004.
(43) Pople, J. A.; Beveridge, D. L.; Dobosh, P. A. *J. Chem. Phys.* **1967**, *47*, 2026.
(44) Mataga, N.; Nishimoto, K. *Z. Phys. Chem.* **1957**, *13*, 140.
(45) Zerner, M. C.; Loew, G. H.; Kichner, R. F.; Mueller-Westerhoff, U. T. *J. Am. Chem. Soc.* **1980**, *102*, 589.
(46) For the ZINDO/MRDCI part, we have fully modified the codes so that the maximum number of CI configurations can exceed the 6000 limit and the high numerical effiency is achieved by implementing Davidson's diagonalization algorithm. This code also requires an identical CI-active space for single and multiple excitations, which has been different in some of our previous studies (see the corresponding methodology sections).
(47) Ridley, J.; Zerner, M. *Theor. Chim. Acta* **1973**, *32*, 111.
(48) Buenker, R. J.; Peyerimhoff, S. D. *Theor. Chim. Acta* **1974**, *35*, 33.
(49) Tavan, P.; Schulten, K. *J. Chem. Phys.* **1986**, *85*, 6602.
(50) Shuai, Z.; Beljonne, D.; Brédas, J. L. *J. Chem. Phys.* **1992**, *97*, 1132.
(51) Orr, B. J.; Ward, J. F. *Mol. Phys.* **1971**, *20*, 513.
(52) Peticolas, W. L. *Annu. Rev. Phys. Chem.* **1967**, *18*, 233.
(53) Zalenśny, R.; Bartowiak, W.; Styrcz, S.; Leszczynski, J. *J. Phys. Chem. A* **2002**, *106*, 4032.
(54) Monson, P. R.; McClain, W. M. *J. Chem. Phys.* **1970**, *53*, 29.
(55) Frisch, M. J.; Trucks, G. W.; Schlegel, H. B.; Scuseria, G. E.; Robb, M. A.; Cheeseman, J. R.; Montgomery, J. J. A.; Vreven, T.; Kudin, K. N.; Burant, J. C.; Millam, J. M.; Iyengar, S. S.; Tomasi, J.; Barone, V.; Mennucci, B.; Cossi, M.; Scalmani, G.; Rega, N.; Petersson, G. A.; Nakatsuji, H.; Hada, M.; Ehara, M.; Toyota, K.; Fukuda, R.; Hasegawa, J.; Ishida, M.; Nakajima, T.; Honda, Y.; Kitao, O.; Nakai, H.; Klene, M.; Li, X.; Knox, J. E.; Hratchian, H. P.; Cross, J. B.; Bakken, V.; Adamo, C.; Jaramillo, J.; Gomperts, R.; Stratmann, R. E.; Yazyev, O.; Austin, A. J.; Cammi, R.; Pomelli, C.; Ochterski, J. W.; Ayala, P. Y.; Morokuma, K.; Voth, G. A.; Salvador, P.; Dannenberg, J. J.; Zakrzewski, V. G.; Dapprich, S.; Daniels, A. D.; Strain, M. C.; Farkas, O.; Malick, D. K.; Rabuck, A. D.; Raghavachari, K.; Foresman, J. B.; Ortiz, J. V.; Cui, Q.; Baboul, A. G.; Clifford, S.; Cioslowski, J.; Stefanov, B. B.; Liu, G.; Liashenko, A.; Piskorz, P.; Komaromi, I.; Martin, R. L.; Fox, D. J.; Keith, T.; Al-Laham, M. A.; Peng, C. Y.; Nanayakkara, A.; Challacombe, M.; Gill, P. M. W.; Johnson, B.; Chen, W.; Wong, M. W.; Gonzalez, C.; Pople, J. A. *Gaussian03*, revision C.02; Gaussian Inc.: Wallingford, CT, 2004.

Science Foundation of China (Grant No. 20420150034) for supporting international cooperation.

Supporting Information Available: Figures showing 1PA and degenerate and nondegenerate 2PA spectra for compounds **1** and **3**−**7** and table comparing Mulliken partial charges on donor portions of the chromophores according to AM1 and DFT calculations and comparing INDO-calculated 1PA transition energies based on AM1 and DFT geometries. This material is available free of charge via the Internet at http://pubs.acs.org.

CM061681L